environmental microbiology

Environmental Microbiology (2014) doi:10.1111/1462-2920.12428

Shifts in microbial community structure and function in light- and dark-grown biofilms driven by warming

Anna M. Romaní,[1]* Carles M. Borrego,[2,3] Verónica Díaz-Villanueva,[4] Anna Freixa,[1] Frederic Gich[2] and Irene Ylla[1]

[1]*Group of Continental Aquatic Ecology,* [2]*Group of Molecular Microbial Ecology, Institute of Aquatic Ecology, University of Girona, Girona, Spain.*

[3]*Water Quality and Microbial Diversity, Catalan Institute for Water Research (ICRA), Girona, Spain.*

[4]*Limnology Laboratory, INIBIOMA-CONICET, Bariloche, Argentina.*

Summary

Biofilms are dynamic players in biogeochemical cycling in running waters and are subjected to environmental stressors like those provoked by climate change. We investigated whether a 2°C increase in flowing water would affect prokaryotic community composition and heterotrophic metabolic activities of biofilms grown under light or dark conditions. Neither light nor temperature treatments were relevant for selecting a specific bacterial community at initial phases (7-day-old biofilms), but both variables affected the composition and function of mature biofilms (28-day-old). In dark-grown biofilms, changes in the prokaryotic community composition due to warming were mainly related to rotifer grazing, but no significant changes were observed in functional fingerprints. In light-grown biofilms, warming also affected protozoan densities, but its effect on prokaryotic density and composition was less evident. In contrast, heterotrophic metabolic activities in light-grown biofilms under warming showed a decrease in the functional diversity towards a specialized use of several carbohydrates. Results suggest that prokaryotes are functionally redundant in dark biofilms but functionally plastic in light biofilms. The more complex and self-serving light-grown biofilm determines a more buffered response to temperature than dark-grown biofilms. Despite the moderate increase in temperature of only 2°C, warming conditions drive significant changes in freshwater biofilms, which responded by finely tuning a complex network of interactions among microbial populations within the biofilm matrix.

Received 28 July, 2013; accepted 9 February, 2014. *For correspondence. E-mail anna.romani@udg.cat; Tel. 34 972 418467; Fax 34 972 418150.

Introduction

Biofilms mediate a significant proportion of the carbon turnover and dominate the ecosystem metabolism in many aquatic systems, being a major component for the uptake, storage and cycling of available organic matter (Pusch *et al.*, 1998; Singer *et al.*, 2010). Among biofilm components, microbial heterotrophs play a key biogeochemical role in stream ecosystems (Findlay, 2010). It is then relevant to discern whether the predicted global change scenarios would affect microbial biofilm structure and function. Specific studies show that temperature significantly affects biofilm metabolism, increasing denitrification rates, primary production and community respiration (Boulêtreau *et al.*, 2012; Perkins *et al.*, 2012). Temperature can also affect biofilm community composition, as has been shown in a field study where temperature was one of the most relevant environmental parameters related to biofilm community composition (Lear *et al.*, 2008). In planktonic habitats, the response of bacteria to warming has been shown to be taxa-specific (Fuhrman *et al.*, 2006). However, most studies include a wider range of temperatures than the 2.2–4.3°C predicted increase in mean river water temperatures for climate change scenarios by 2100 (Mohseni and Stefan, 1999; IPCC, 2007). Ylla and colleagues (2012) showed that the activity of biofilm extracellular enzymes was enhanced after a 4°C increase in response to dissolved organic carbon quality and availability. In turn, 4°C temperature increases may not affect the composition of bacterial planktonic communities unless nutrient concentration also increases (Degerman *et al.*, 2013).

The response of the prokaryotic community composition and functioning to 2–4°C increase might be sensitive to the interaction with other biofilm components, which may modify the biofilm microenvironment (i.e. changing resource availability and grazing). The role of biofilm interactions was shown in a previous study, where although an increase in 3°C determined a faster accrual of bacteria, the total bacterial biomass at the mature biofilm remained fairly constant due to a larger ciliate grazing pressure, and no significant effect on extracellular enzyme activities was

found (Díaz-Villanueva *et al*., 2011). Interactions in the biofilm became very different depending on the existence – or not – of primary producers. Under illumination conditions, such as those in the upper side of cobbles from open streams, autotrophic biofilms densely grow, reaching algal abundances of up to 60–90% of total biomass (Romaní, 2010). The accrual of algal and cyanobacterial biomass increases the dependency of heterotrophic bacteria on organic carbon supplied by primary producers (Neely and Wetzel, 1995; Ziegler *et al*., 2009), stimulating the selection of photoautotrophic-dependent bacteria (Watanabe *et al*., 2008). Primary producers not only provide direct available organic matter sources for heterotrophs but also produce a priming effect on the decomposition of other more complex organic substrates (Guenet *et al*., 2010). In general, the availability of algal resources also increases ciliate densities and stimulates specific ciliate groups that feed upon biofilm surface (Früh *et al*., 2011). In contrast, under dark conditions, such as those present under stream cobbles or within hyporheic zones or in pipes, biofilms are thinner, contain low bacterial biomass and exhibit a greater dependence on changes in dissolved organic matter in flowing water (Romaní *et al*., 2004). Light and dark conditions also affect the composition of prokaryotic communities in biofilms. Dark-grown biofilms had a lower bacterial diversity dominated by *Actinobacteria* and *Betaproteobacteria*, whereas a higher diversity, including *Actinobacteria*, *Alpha-*, *Beta-* and *Gammaproteobacteria*, *Gemmatimonadetes*, and *Cyanobacteria*, was found in light-grown biofilms (Romaní *et al*., 2004; Ylla *et al*., 2009). Moreover, higher abundance of ammonia-oxidizing archaea was found in the dark side of river cobbles rather than on illuminated sides, a segregation that agrees with their photosensitivity (Church *et al*., 2010; Merbt *et al*., 2011).

Heterotrophic functioning and prokaryotic community composition may not respond equally when changing the environment (Langenheder *et al*., 2005), as observed in a pioneering community developing on streambed biofilms (Frossard *et al*., 2012). It has also been shown that functional capabilities are not always necessarily linked to community composition since they might depend on their metabolic plasticity (Comte and del Giorgio, 2011), although the capacity of biofilms to use a wider range of organic substances might be linked to its community diversity (Peter *et al*., 2011).

The aim of this study was to investigate how an increase of temperature by 2°C would affect the prokaryotic community composition, abundance and heterotrophic function in biofilms grown under light and dark conditions. This minor temperature increase relies in the lower range of predicted temperature change, and it will provide a more realistic approach on structural and functional variations in biofilms subjected to warming. We specifically addressed whether (i) the prokaryotic community composition would change according to heterotrophic functioning responses, (ii) the prokaryotic responses would be modulated by the differential development of other microbial groups in the biofilm (algae, ciliates, rotifers) and (iii) the response would be different at initial stages of biofilm formation (young biofilms, 7 days old) than at final stages (mature biofilms, 28 days old). For this purpose, biofilm colonization was analysed in laboratory microcosms submitted to four different treatments: light-low temperature (L-LT), light-high temperature (L-HT), dark-low temperature (D-LT) and dark-high temperature (D-HT). The low temperature corresponded to the mean ambient stream temperature where the biofilm inoculum was collected (mean of 14.6°C) and high temperature corresponded to a 2°C increase from that temperature (mean of 16.6°C). Light conditions consisted of a natural day–night cycle (12 h/12 h), and dark conditions consisted of total darkness. Biofilm formation on 1 cm^2 sand-blasted glass tiles was analysed in terms of biomass accrual (algal, bacterial, ciliate, rotifer), prokaryote function (extracellular enzyme activities and carbon substrate utilization profiles) and prokaryote community composition [denaturing gradient gel electrophoresis (DGGE) and pyrosequencing].

Results

Light and temperature effects on microbial biofilm colonization

Chlorophyll-*a* concentration in the colonizing biofilms was positively affected by light (Fig. 1A). At the end of biofilm colonization (days 28 and 34), temperature further enhanced chlorophyll accrual in light conditions (Fig. 1A, Table 1).

Ciliate densities along biofilm colonization were positively affected by light, but this was mainly due to increased densities under L-LT conditions at the end of the experiment (Fig. 1B, Table 1). At the end of biofilm colonization, ciliate density increased under low-temperature conditions, showing a peak on day 28 (in D-LT) and on day 34 (in L-LT), while ciliate densities at all high temperature treatments were maintained at low values (Fig. 1B, Table 1, day × temperature effects). In contrast, colonization of biofilms by rotifers was significantly enhanced by temperature (Fig. 1C, Table 1).

Prokaryote densities over time were positively affected by light (Fig. 1D, Table 1, light and day × light effects). At the end of biofilm colonization (day 28), temperature exerted a negative effect on prokaryote density (Fig. 1, Table 1, day × temperature effects). The significant interaction of temperature and light indicated

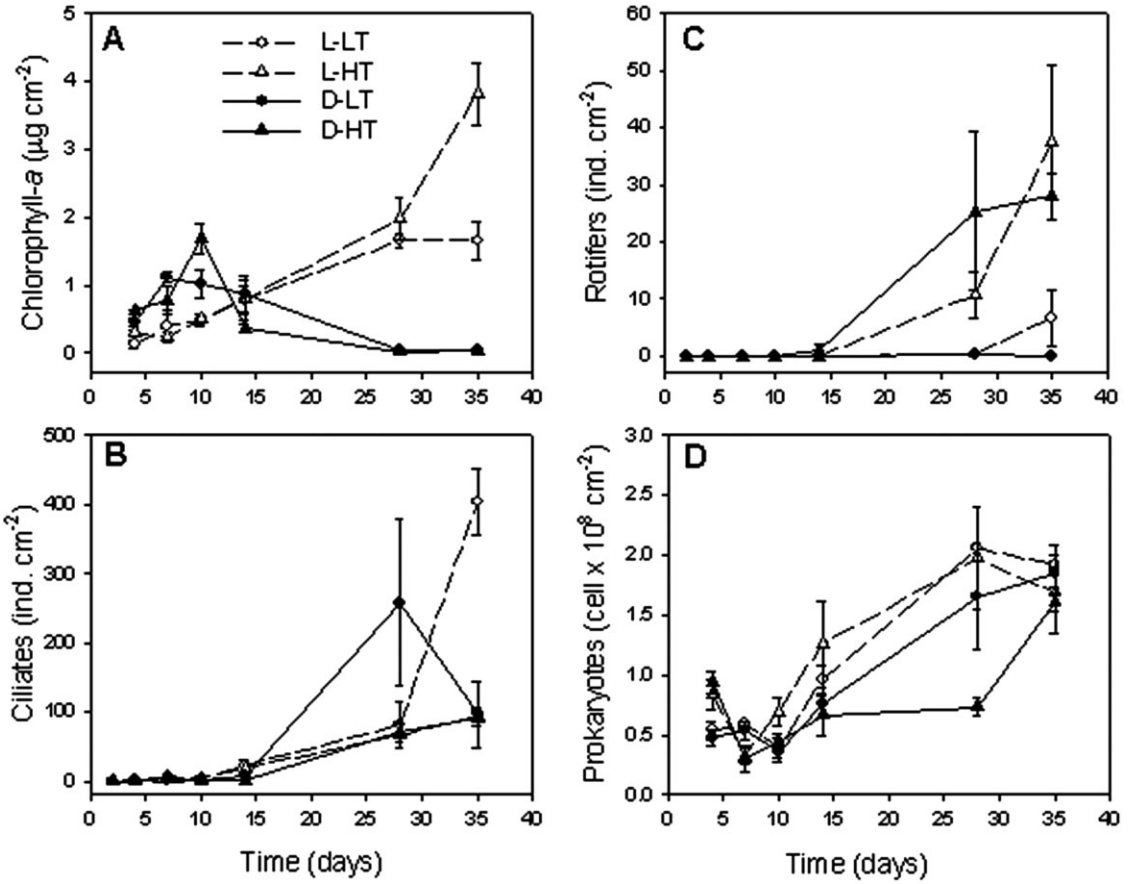

Fig. 1. Temporal development of chlorophyll-a, prokaryotes, ciliates and rotifers density during biofilm colonization for the different treatments (L: light; D: dark; LT: low temperature; HT: high temperature). Values are means ± SE ($n = 3$).

that the negative effect of warming on prokaryotes was more pronounced under dark conditions (Fig. 1, Table 1).

Illumination also had a significant effect on 16S rRNA gene copy numbers of bacteria and archaea (*Crenarchaeota*-*Thaumarchaeota*), especially in mature biofilms (Fig. 2, Table 2). Also, the ratio of archaeal to bacterial 16S rRNA gene copy numbers was significantly higher in young biofilms (Fig. 2, Table 2). Bacterial and archaeal 16S rRNA gene copy numbers were also

Table 1. Results from the repeated measures analyses of variance showing the effect of dark/light (L) and temperature (T) on biofilm structure and function parameters analysed throughout the biofilm colonization processes.

Source of variation	Chlorophyll-*a*	Prokaryotes	Ciliates	Rotifers	β-glucosidase	Phosphatase	Peptidase
Day	***0.002***	< **0.001**	< **0.001**	< **0.001**	< **0.001**	< **0.001**	< **0.001**
	(2.1,16.9)	*(2.8,22.9)*	*(2.4,18.9)*	*(2.4,18.9)*	*(3.5,28.4)*	*(1.9,15.5)*	*(2.5,20.4)*
L	< ***0.001***	< **0.001**	*0.066*	0.71	< **0.001**	**0.020**	< **0.001**
	(1,8)	*(1,8)*	*(1,8)*	*(1,8)*	*(1,8)*	*(1,8)*	*(1,8)*
T	*0.071*	**0.032**	0.23	< **0.001**	0.28	0.55	0.17
	(1,8)	*(1,8)*	*(1,8)*	*(1,8)*	*(1,8)*	*(1,8)*	*(1,8)*
Day × L	< ***0.001***	*0.053*	*0.055*	*0.099*	< **0.001**	*0.075*	< **0.001**
	(2.1,16.9)	*(2.8,22.9)*	*(2.4,18.9)*	*(2.4,18.9)*	*(3.5,28.4)*	*(1.9,15.5)*	*(2.5,20.4)*
Day × T	***0.028***	< **0.001**	**0.020**	< **0.001**	**0.047**	0.18	0.15
	(2.1,16.9)	*(2.8,22.9)*	*(2.4,18.9)*	*(2.4,18.9)*	*(3.5,28.4)*	*(1.9,15.5)*	*(2.5,20.4)*
L × T	***0.025***	**0.011**	0.69	*0.084*	0.69	0.78	**0.010**
	(1,8)	*(1,8)*	*(1,8)*	*(1,8)*	*(1,8)*	*(1,8)*	*(1,8)*
Day × L × T	*0.066*	0.11	0.19	0.35	0.16	0.74	0.26
	(2.1,16.9)	*(2.8,22.9)*	*(2.4,18.9)*	*(2.4,18.9)*	*(3.5,28.4)*	*(1.9,15.5)*	*(2.5,20.4)*

Probability within groups (day and interactions day × L, day × T, and day × L × T) is corrected for sphericity by the Greenhouse-Geisser correction. Degrees of freedom for F-ratios are also indicated in italics, and parenthesis. The significant probabilities are shown: < 0.05 in bold, < 0.1 in italics.

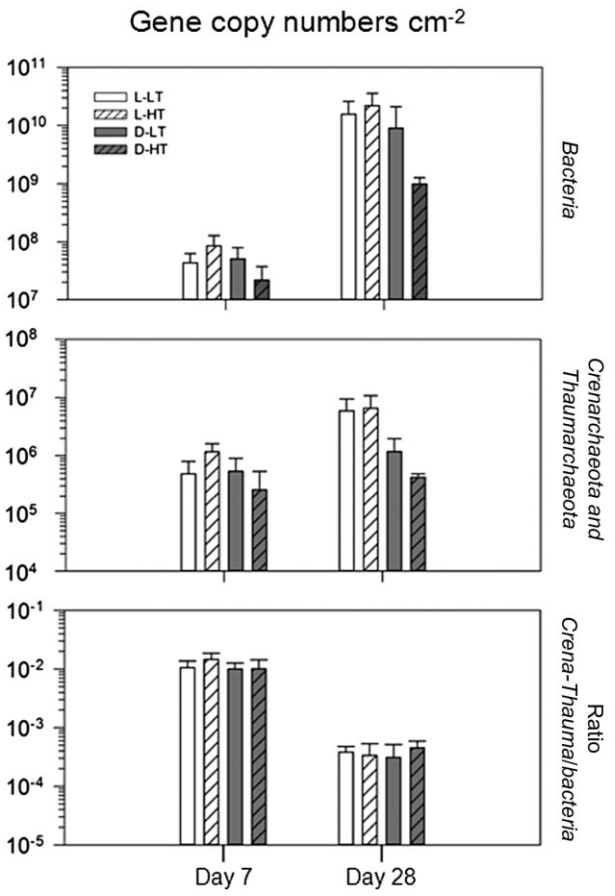

Fig. 2. Gene copy numbers for *Bacteria* and *Crenarchaeota* and *Thaumarchaeota*, and ratio between gen copies of *Crenarchaeota* and *Thaumarchaeota v. Bacteria* for biofilms collected after 7 days (young) and 28 days (mature) of incubation under the imposed treatments (L: light; D: dark; LT: low temperature; HT: high temperature). Values are means ± SE ($n = 3$).

negatively affected by warming under dark conditions (Fig. 2, Table 2, light × temperature effects).

Light and temperature effects on prokaryote biofilm community composition

Samples from each triplicated treatment yielded identical band patterns that were indicative of the reproducibility of the experimental design. After 7 days of incubation, fingerprints of bacterial 16S rRNA gene were highly similar for all treatments but differed from the indigenous community used as inoculum (Fig. S1). This homogeneous composition in young biofilms changed after 28 days of incubation, where clearly different fingerprints were observed for biofilms grown under light and dark conditions. Effects of warming were in turn hardly visible from DGGE fingerprints. BLAST search of sequences recovered from discrete bands showed a dominance of *Alphaproteobacteria* in the inoculum sample, *Betaproteobacteria* in young biofilms, and *Cyanobacteria*, *Actinobacteria* and *Proteobacteria* in 28-day-old biofilms (Table S1). As expected, most sequences obtained from biofilms incubated under light conditions affiliated within the *Cyanobacteria* (Table S1 and Fig. S1).

The low number of bands observed in most fingerprints suggested bacterial communities characterized by low richness, although known limitations of the DGGE technique surely contributed (Muyzer and Smalla, 1998). To overcome this limitation, DNA samples from mature biofilms were subjected to massively parallel sequencing using 454 technology to have a deeper insight of potential changes induced by light and warming on biofilm bacterial communities. After denoising and filtering for quality, the final pyrosequencing dataset consisted in 14 108 sequences (1701 dereplicated sequences) that, on average, distributed by 2846 reads per sample (min = 1670, max = 5268, SD = 1350) with an average length of 494 nt (min = 225, max = 550). This sampling effort was sufficient to capture most of the bacterial diversity as indicated by rarefaction plots (not shown). Maximum diversity was measured for the inoculum and decreased in all treatments (Table S2). Clustering of sequences into operational taxonomic units (OTUs) at 97% cut-off resulted in 496 OTUs across samples. Most of these OTUs were classified at the class and family levels at a confidence threshold > 90%. The largest fraction of OTUs (278 out of 496, 56.1%) affiliated within the *Proteobacteria*, and they were distributed in 163, 52, 42 and 15 OTUs within classes *Alpha-*, *Beta-*, *Delta-* and

Table 2. Results from the three-way ANOVA [factors light (L), temperature (T) and day] for the parameters measured at the young biofilms (day 7) and old biofilms (day 28).

Source of variation	Gene copy Bacteria	Gene copy Crena-Thauma	Ratio gene copy Crena-Thauma/Bacteria	Functional diversity	Functional richness
Day	< **0.001**	< **0.001**	< **0.001**	< **0.001**	< **0.001**
L	**0.001**	< **0.001**	0.24	0.83	0.64
T	0.39	0.69	0.33	0.99	0.77
Day × L	*0.053*	*0.070*	0.23	*0.060*	*0.99*
Day × T	0.57	0.58	0.35	*0.066*	0.39
L × T	**0.028**	**0.042**	0.38	0.46	0.11
Day × L × T	0.88	0.45	0.33	**0.045**	0.082

Degrees of freedom for F-ratios are 1, 16. The significant probabilities are shown: < 0.05 in bold, < 0.1 in italics.

Gammaproteobacteria respectively. The phylum *Bacteroidetes* (55 OTUs), *Cyanobacteria* (71 OTUs) and *Actinobacteria* (32 OTUs) grouped most of the remaining diversity. OTUs affiliated to rare taxa accounted for 8% of the total, whereas only 4% of OTUs remained unclassified (Table S3). The analysis of bacterial community composition among treatments revealed a clear dominance of sequences affiliated to *Cyanobacteria* and *Alphaproteobacteria* in biofilms exposed to light conditions despite temperature regime (Fig. 3). In turn, biofilms grown under dark conditions showed the most dissimilar bacterial communities, with a dominance of *Proteobacteria*. Particularly, sequences affiliated to class *Alphaproteobacteria* were predominant in the inoculum samples as well as in biofilms incubated in D-LT, whereas *Gammaproteobacteria* were the most abundant bacterial class in biofilms incubated in D-HT. These trends were also observed when only the relative contribution and taxonomic affiliation of most populated OTUs (> 100 members) were considered (Fig. 3). Abundance-filtered OTU data revealed not only the important contribution of *Cyanobacteria* in illuminated biofilms but also the prevalence of *Alphaproteobacteria* in all samples despite light regime and temperature. Besides, most alphaproteobacterial OTUs that were prevalent in the inoculum sample decreased their relative abundance in the experimental treatments (Fig. 3). Interestingly, only two OTUs (OTU-277 and OTU-286) showing high pairwise identity to *Vibrio* species grouped most of the sequences affiliated to *Gammaproteobacteria* that characterized the bacterial community developed in biofilms incubated at high temperature in the dark (D-HT).

Clustering of samples according to their weighted phylogenetic distances (weighted UniFrac) grouped bacterial communities from illuminated biofilms apart from the remaining treatments as a result of the abundance of cyanobacterial sequences under light conditions (Fig. 3). When no quantitative correction was used (unweighted UniFrac), clustering clearly separated the inoculum community from the rest of samples, which further segregated D-HT community from the rest (Fig. S2A). To unveil hidden associations between samples potentially masked by the predominance of cyanobacterial sequences in biofilms incubated under illumination (particularly L-HT), clustering analysis was repeated after filtering cyanobacterial OTUs (71 out of 500) from the dataset. In this case, biofilms incubated under high temperature in the dark (D-HT) clearly separated from the rest of treatments, whereas samples from illuminated biofilms clustered together using both weighted and unweighted phylogenetic distances (Fig. S2B).

To compare to what extent the molecular approaches used (i.e. pyrosequencing and DGGE) were able to identify differences in the composition of bacterial biofilm communities across treatments, the relative abundance of taxa calculated from pyrotags was compared with differences in band fingerprints according to the Bray–Curtis similarity index. Although samples from illuminated biofilms grouped together despite the molecular approach used, the overall clustering is clearly affected by their different resolution (Fig. S3). This can be partially explained by the predominance of cyanobacterial sequences in DGGE fingerprints and the low number of sequences affiliated to other taxa (Table S1). Besides, the differences in the dataset used to calculate Bray–Curtis similarity (quantitative for pyrotags and qualitative for DGGE) could be also responsible for the divergent grouping. Nevertheless, many sequences recovered from DGGE fingerprints showed high pairwise identity (≥ 97%) with representative sequences of the 22 most populated OTUs (> 100 members) and grouped together in the phylogenetic tree (Fig. S4).

DGGE fingerprints of archaeal 16S rRNA gene showed few bands that persisted along incubation time with no differences by treatment (Fig. S5). This similarity suggested a stable archaeal community in biofilms characterized by low richness, although this interpretation should be done with caution according to the poor resolution of the fingerprints obtained. Despite the presence of smeary bands, all of them yielded sequences of good quality that affiliated to *Thaumarchaeota* of the Soil Group I.1b that further clustered into 5 OTUs (Table S4). Altogether, these results suggested a low contribution of archaea to total microbial biomass in biofilms, agreeing with the lesser abundance of *Crenarchaeota-Thaumarchaeota* 16S rRNA gene copies in relation to bacterial gene counts (Fig. 2). Accordingly, we considered that most of the archaeal diversity in the biofilms was captured and no further analysis was carried out.

Light and temperature effects on microbial biofilm functions

The activity of extracellular enzymes involved in the use of carbon, nitrogen and phosphorus organic compounds was enhanced in biofilms growing under illumination (Fig. 4, Table 1). Although temperature as a single factor did not affect any of the extracellular enzymes, activity of β-glucosidase was significantly lower in warmer treatments at the end of biofilm colonization (Table 1, day × temperature effect). Concerning leucine-aminopeptidase, warming conditions stimulated its activity in illuminated biofilms (L-HT) while the opposite effect was observed in biofilms incubated under dark conditions (Table 1, light × temperature effect).

The capacity of biofilm communities to use diverse organic compounds showed very similar results for young biofilms from all treatments, and was characterized by the use of glycogen and L-asparagine (Table 3, Fig. 5). In

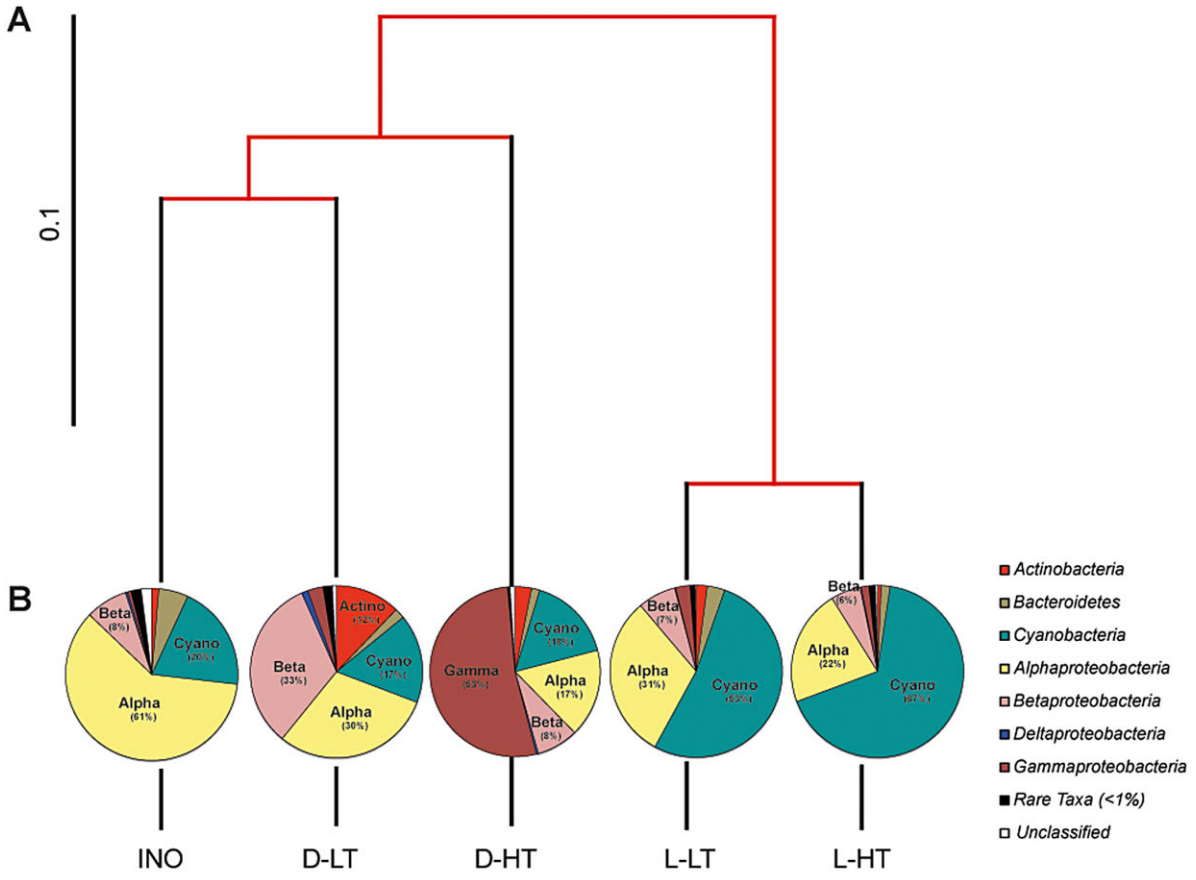

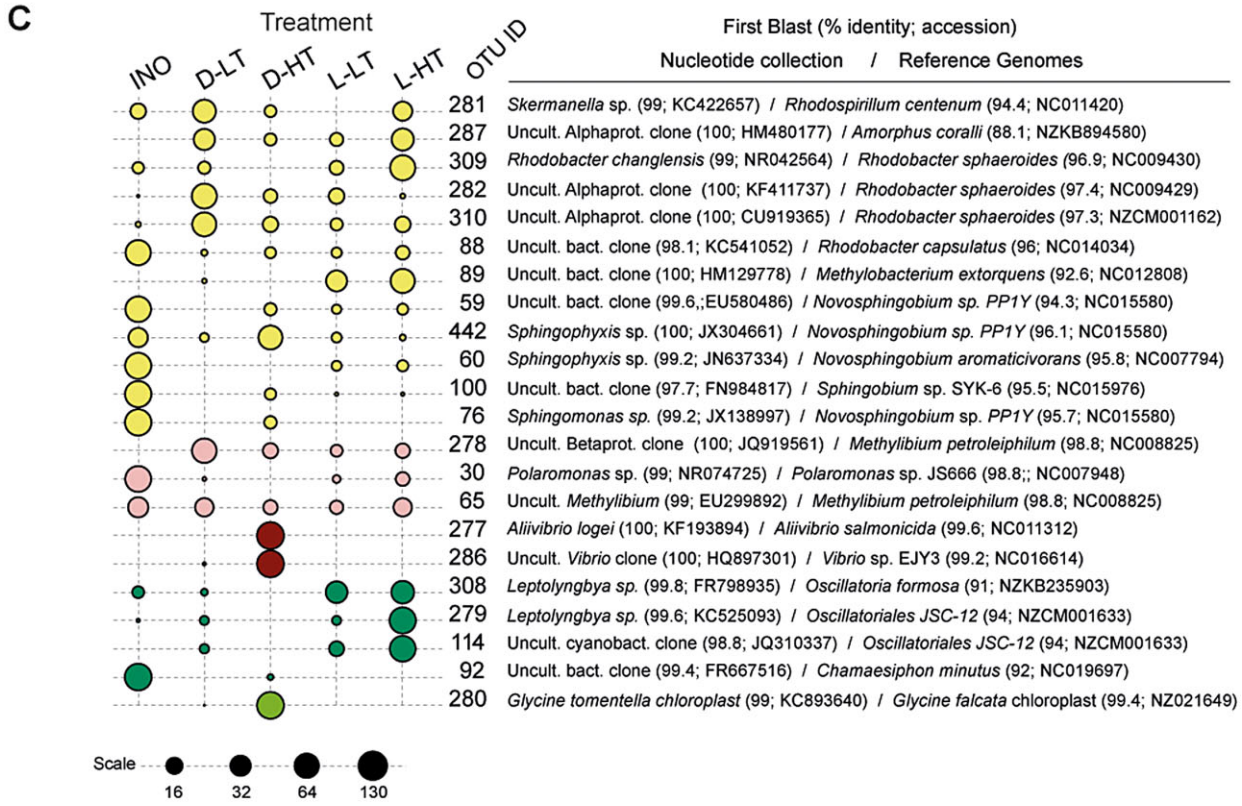

Fig. 3. Clustering of samples according to bacterial community similarity with relative abundances of main bacterial phyla/classes and heatmap of OTU abundances across sample treatments.
A. Top dendrogram was built using weighted UniFrac distances calculated after phylogenetic analysis of pyrosequencing data from bacterial communities in mature biofilms (28 days old).
B. Pie charts display the relative abundance of pyrotag sequences affiliated to main bacterial phyla (classes within the *Proteobacteria*) in each treatment. Phyla with relative abundances below 1% were grouped together and considered as rare taxa.
C. Bubble plot at the bottom displays the relative abundance of most populated OTUs (≥ 100 members) across samples. Data values are proportional to radius and plotted in a logarithmic scale as indicated below the graph. Taxa are colour-coded as follows: *Alphaproteobacteria* (yellow), *Betaproteobacteria* (pink), *Gammaproteobacteria* (dark red), *Cyanobacteria* (dark green), chloroplasts (light green).

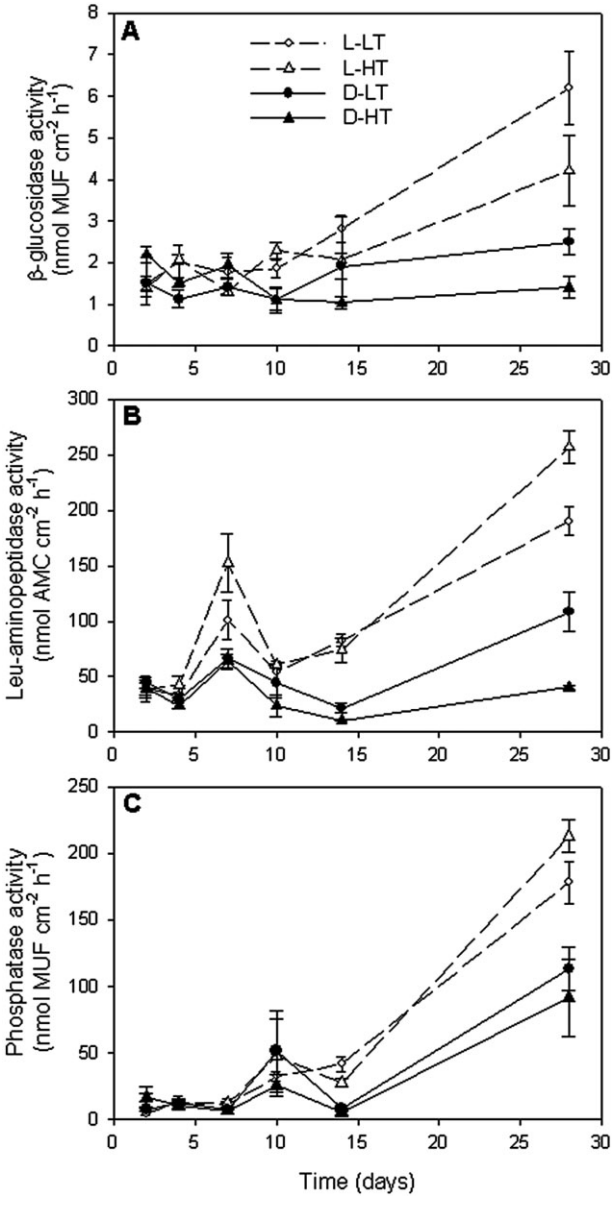

Fig. 4. Temporal development of extracellular enzyme activities during biofilm colonization for the different treatments (L: light; D: dark; LT: low temperature; HT: high temperature). Values are means ± SE ($n = 3$).

contrast, similarity between all mature biofilms decreased mainly due to the separation of L-HT biofilms (Fig. 5, Table 3). Functional diversity and richness were significantly reduced over time (from young to mature biofilms, Tables 2 and 4) mostly due to the loss of biofilm community capacity to use some amino acids, carbohydrates and carboxylic acids (Table 3). Mature biofilms in L-LT and L-HT showed a large dissimilarity between their functional fingerprints (39%, Table 3). Biofilms grown under L-LT conditions were specially characterized by the use of amino acids (L-asparagine and L-serine), while L-HT biofilms showed a significant decrease in functional diversity (Table 3, Table 2 day × temperature effect) and a metabolic specialization on the use of D-mannitol (Table 3). Also, in L-HT biofilms, there was less similarity between replicates (Fig. 5, Table 3). The microbial community under dark conditions was characterized using carboxylic acids and polymers (Table 3), and the effect of warming was less evident (Fig. 5). D-LT and D-HT biofilms showed low dissimilarity between their functional fingerprints (25.8%), and this was mainly due to a major capability to use some carboxylic acids at the D-LT biofilm (Table 3). In dark biofilms, warming caused a slight increase in functional richness and diversity (Table 4).

The photosynthetic efficiency of light-grown mature biofilms decreased significantly due to imposed warming (from 0.37 ± 0.014 to 0.27 ± 0.017 in L-LT and L-HT treatments respectively, $P = 0.009$). Warmer conditions determined a greater contribution of diatoms versus green algae, and a greater contribution of *Cyanobacteria* versus green algae (significant increase in the F1/F2 and F1/F3 fluorescence ratios, $P < 0.05$). As expected, no photosynthetic activity was detected in biofilms incubated in darkness.

Relationships between prokaryote community composition and biofilm function and structure

The relationships between prokaryote community composition and biofilm function and structure were shown by redundancy analyses, which explained 70.3% and 21.1% of variance, respectively, for axis 1 and axis 2 (Fig. 6). In D-HT, the abundance of rotifers was related to most common OTUs found in D-HT biofilms, especially those affiliated to *Vibrionaceae* (OTU-277 and OTU-286). In D-LT biofilms, the abundance of ciliates was associated

Table 3. Characteristic organic substrates being used by each biofilm after the SIMPER analysis.

Day 7 versus day 28		Day 7 *85.43 % avg. sim.*	Day 28 *67.39% avg. sim.*	Day 7 versus day 28 *36.31% avg. diss*
C substrates	Type of substrate	% Contribution to average similarity		% Contribution to average dissimilarity
Glycogen	*Polymer*	11.49	*(2.88)*	10.49
Tween 80	*Polymer*	5.31	11.09	6.88
Tween 40	*Polymer*	*(4.46)*	6.81	5.37
L-Asparagine	*Amino acid*	9.72	8.72	
D-Galacturonic acid	*Carboxylic acid*	*(4.50)*	13.16	8.15
D-Malic acid	*Carboxylic acid*	5.50		
D-Mannitol	*Carbohydrate*	5.14	9.66	7.11
N-acetyl-D-glucosamine	*Carbohydrate*	5.92		
β-methyl-D-glucoside	*Carbohydrate*	4.80	*(0.30)*	5.58
Day 28 light		L-LT *78.35% avg. sim.*	L-HT *62.72% avg. sim.*	L-LT versus L-HT *39.07% avg. diss*
Tween 80	*Polymer*	7.81	11.20	8.41
Tween 40	*Polymer*	*(3.05)*	*(9.46)*	9.55
L-Asparagine	*Amino acid*	14.06	*(3.25)*	9.50
L-Serine	*Amino acid*	7.91	*(0.04)*	9.06
D-Galacturonic acid	*Carboxylic acid*	11.78	14.08	
D-Mannitol	*Carbohydrate*	9.12	24.47	11.23
Day 28 dark		D-LT *77.55% avg. sim.*	D-HT *72.56% avg. sim.*	D-LT versus D-HT *25.81% avg. diss.*
Tween 80	*Polymer*	11.71	10.54	6.69
Tween 40	*Polymer*	7.29	8.32	7.78
L-Asparagine	*Amino acid*	8.34	9.35	
D-Galacturonic acid	*Carboxylic acid*	12.90	9.71	8.86
Pyruvic acid methyl ester	*Carboxylic acid*	8.78	*(4.80)*	6.31
D-Malic acid	*Carboxylic acid*		7.64	

Differences are shown for young (day 7) versus mature (day 28) biofilms, L-LT versus L-HT, and D-LT versus D-HT biofilms. The organic substrates contributing up to 50% of total average similarity between samples (avg. sim.) and until 5% of average dissimilarity (avg. diss.) between the compared treatments are listed. The similarity values in italics and parentheses correspond to those substrates not contributing to the first 50% similarity but significantly contributing to dissimilarity.

with 3 OTUs affiliated to purple non-sulfur bacteria within *Alphaproteobacteria* and 1 OTU (OTU-278) represented by an uncultured Betaproteobacterium (Fig. 6A).

When considering the relationship between prokaryote community composition and carbon substrate utilization profiles, the use of carbohydrates was clearly linked to several OTUs prevalent in L-HT biofilms, including two OTUs affiliated to *Alphaproteobacteria* (OTU-89 and OTU-309) and three cyanobacterial OTUs (OTU-114, OTU-308 and OTU-279, Fig. 6B). A significant correlation

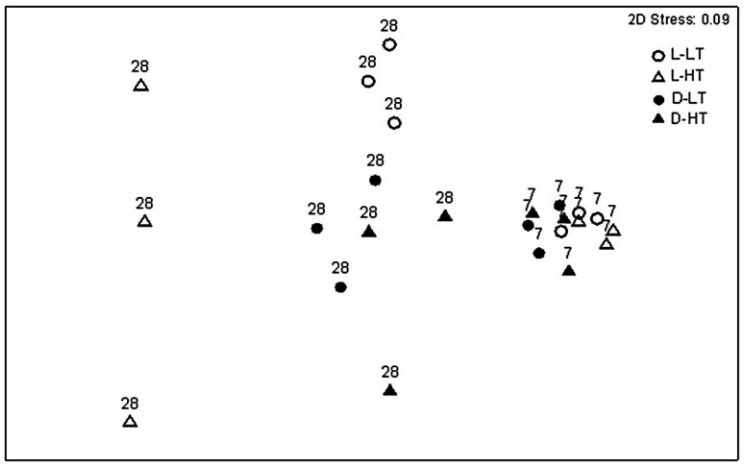

Fig. 5. Non-metric multidimensional scaling (nMDS) ordination of potential organic matter use capabilities of 31 carbon substrata of young (7 days old) and mature (28 days old) biofilms from the four imposed treatments (L: light; D: dark; LT: low temperature; HT: high temperature). Kruskal 2D stress is shown.

Table 4. Richness and diversity of heterotrophic metabolic activities for the young (day 7) and old (day 28) biofilms grown under the different treatments.

	Light		Dark	
	Low temp	High temp	Low temp	High temp
Richness (positive wells)				
Day 7	29.3 ± *1.52*	30.7 ± *0.57*	30 ± *1.73*	31 ± *0*
Day 28	26.7 ± *1.52*	23.3 ± *3.78*	24 ± *1*	26.7 ± *3.21*
Diversity (Shannon)				
Day 7	3.1 ± *0.03*	3.3 ± *0.35*	3.1 ± *0.05*	3.1 ± *0.03*
Day 28	2.9 ± *0.09*	2.6 ± *0.13*	2.8 ± *0.06*	2.9 ± *0.21*

The mean values ± standard deviation (in italics) are indicated ($n = 3$).

was found between OTU-309, OUT-30 and OTU-114 and the use of D-mannitol ($P < 0.03$). Although carboxylic acids were not linked to any specific OTU, the correlation of all carbon substrates to prokaryote community composition yielded significant correlations between D-glucosaminic acid and OTU-308 ($P = 0.023$) and α-ketobutyric acid with OTU-309, OTU-114 and OTU-279 ($P < 0.02$) mainly found in L-HT biofilms (Fig. 6B).

Scanning electron microscope (SEM) observations

Scanning electron microscopy photographs of 28-day-old biofilms showed clear differences between biofilms grown under dark and light conditions (Fig. 7). Whereas dark-grown biofilms showed no structured matrix, illuminated biofilms showed a complex matrix composed of filamentous algae and bacteria, especially in L-LT biofilms (Fig. 7).

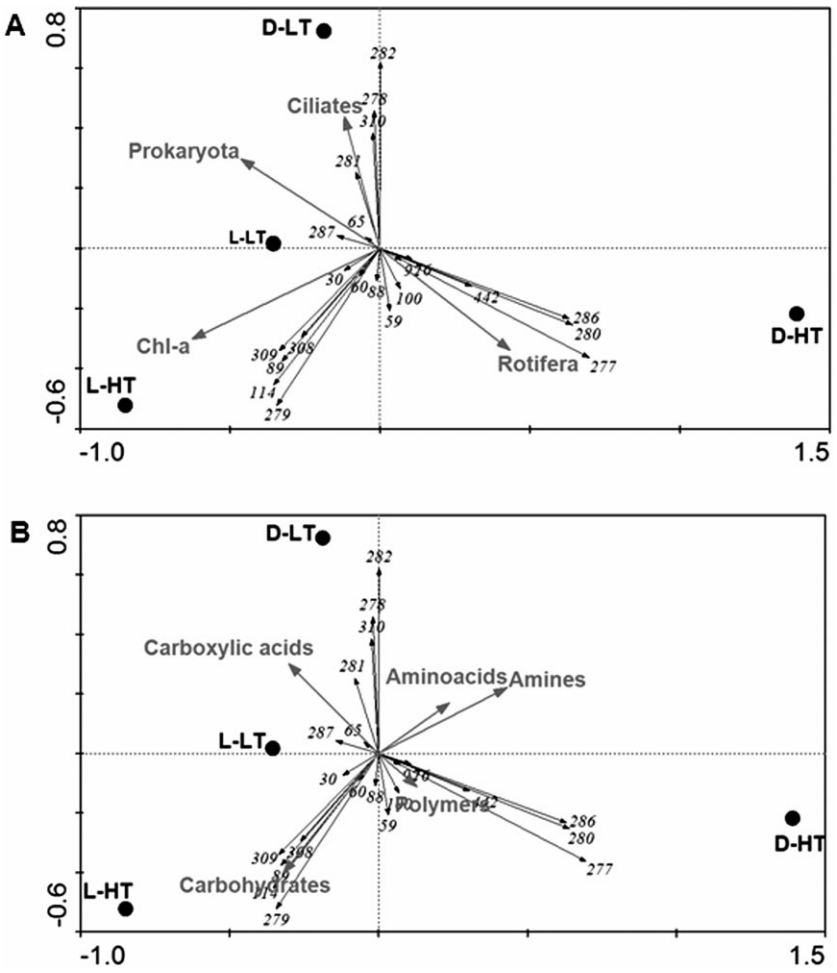

Fig. 6. Triplot based on redundancy analysis (RDA) of the relative abundance of most populated OTUs (≥ 100 members) for each treatment.
A. Ordination plot of density of different biofilm groups (chlorophyll-a, prokaryotes, ciliates and rotifers).
B. Ordination plot with the five groups of carbon substrates from Biolog Ecoplates, in mature biofilms (28 days old). Letters represent different treatments (L: light; D: dark; LT: low temperature; HT: high temperature). Taxonomic affiliation of each OTU identification number is defined in Fig. 3.

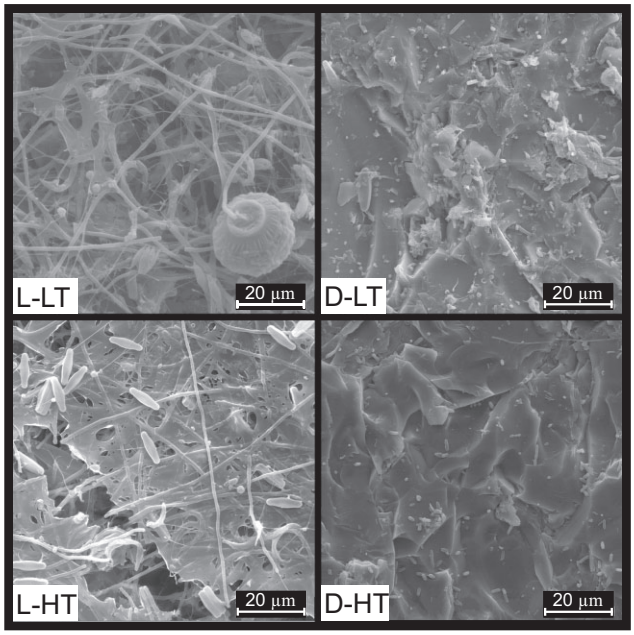

Fig. 7. SEM photographs of 28-day-old biofilms grown in different experimental treatments. A complex matrix of filaments, diatoms and free algal cells can be seen in L-LT biofilms together with *Vorticella* like protozoan. More sparse filaments were observed in L-HT biofilm samples. Biofilms grown under warming and in the dark had lower bacterial densities.

Discussion

It is widely accepted that ecosystems are affected by climate change (Walther *et al*., 2002). Temperature is one of the major factors affecting key biological processes, such as respiration, growth, metabolic rate and feeding (e.g. Hester and Doyle, 2011). In river and streams, increasing temperatures enhance biofilm primary production and respiration (Boulêtreau *et al*., 2012; Rosa *et al*., 2013). The present study significantly improves our knowledge of global warming effects on aquatic biofilms by (i) reporting a response of the biofilm to a realistic temperature increase of 2°C, and (ii) including a wide range of structural and functional biofilm response parameters. Specifically, we found significant differences between the temperature response of young and old biofilms, and in the latter a differential response in both biofilm structure and biofilm function under light and dark conditions.

Young biofilms not affected by light and temperature

In young biofilms (7 days old), neither the structure (microbial biomass, prokaryote community composition) nor the functioning (extracellular enzymes, carbon substrate utilization profile) was affected by light or warming. Young biofilms showed no differences on prokaryotic community composition among treatments, although they clearly diverged from the inoculum (Fig. S1). These first stages of development were characterized by a predominance of *Betaproteobacteria* and higher ratios of archaea/bacteria 16S rRNA gene copy numbers (Fig. 2). This may indicate some selection of species towards those that specifically assemble and begin biofilm formation (Besemer *et al*., 2012; Wey *et al*., 2012), although the experimental system itself might exert some selection. However, gene copy number ratios have to be taken with caution since gene abundances do not necessarily correlate to cell abundances due to multiple ribosomal RNA operon copies in most bacterial genomes (Klappenbach *et al*., 2001). The potential role of archaea as pioneering species at initial stages of biofilm formation is intriguing and deserves future investigation. Studies dealing with archaeal biofilms are scarce and mostly focus on either thermophilic *Crenarchaeota* in thermal springs (Henneberger *et al*., 2006; Pagé *et al*., 2008; Schopf *et al*., 2008) or Euryarchaeota in the human body (Vianna *et al*., 2008). Very few data are available for streambed biofilms, and only Merbt and coworkers recently reported high ratios of AOA/AOB from *amoA* gene abundances at the beginning of biofilm formation on the surface of streambed cobbles (Merbt *et al*., 2011).

Young biofilms also appeared to be less specialized in the use of organic carbon sources as indicated by higher heterotrophic functional richness and diversity when compared with mature biofilms (Table 4). A broad capacity in the use of organic matter might be considered advantageous for pioneering species in terms of competition for the use of available resources (Jackson, 2003). Overall, the metabolic fingerprint in young biofilms was not affected by the imposed treatments (Fig. 5). Glycogen was the most characteristic organic substrate used, which may indicate a significant consumption of intracellular storage compounds during first stages of biofilm formation.

Temperature effects on dark-grown biofilms

Mature biofilms exhibited clear differences in densities of the different trophic groups (Fig. 1). Under dark conditions, the 2°C increase enhanced colonization of the biofilm by rotifers, but decreased the density of ciliates and prokaryotes (Fig. 1 and Fig. 6). The reduced prokaryote density in D-HT biofilms is also shown by the SEM images (Fig. 7). Pajdak-Stós and Fialkowska (2012) observed that increasing temperature by 5°C (from 15 to 20°C) caused a twofold increase of rotifer abundance in biofilms. Ciliate densities might be also enhanced by temperature (Norf *et al*., 2007; Díaz-Villanueva *et al*., 2011). However, if rotifers feed upon bacteria (Ricci and Balsamo, 2000), they may outcompete ciliates and/or directly prey upon ciliates (Gilbert and Jack, 1993),

masking the possible effect of temperature on ciliates. In fact, warming increases the effectiveness of bacteria removal by rotifers (Pajdak-Stós and Fialkowska, 2012). Other authors have found that rotifers exert a top-down control on bacteria and ciliates in 6-week-old biofilms (Augspurger *et al*., 2008).

The biofilm structural changes discussed above determine changes in the prokaryotic community composition of mature biofilms. There was a significant difference in the bacterial community composition from low to high temperature treatments in the dark. The high percentage of sequences affiliated to *Gammaproteobacteria* in D-HT biofilms is somehow surprising according to the low representativeness of this class in the rest of treatments. This anomaly may be related to the abundance of rotifers in D-HT biofilms according to (i) the high pairwise similarity of most gammaproteobacterial sequences from this sample (OTU-277 and OTU-286) to 16S rRNA gene sequences from Vibrios associated to rotifera (e.g. *Vibrio rotiferianus*, Gomez-Gil *et al*., 2003; Ishino *et al*., 2012), and (ii) the high number of *Brachionus* sp. observed during microscope counting in this biofilm (data not shown). The high number of 16S rRNA operon copies in genomes from Vibrios (12 copies on average, Klappenbach *et al*., 2001) hampers drawing conclusions about the actual significance of the high abundance of this bacterial class in D-HT biofilms. Further compositional changes in this biofilm point towards the establishment of a simpler bacterial community due to grazing pressure in D-HT. This would be related to the lower contribution of *Betaproteobacteria* and the presence of pioneering biofilm colonizers, such as *Sphingomonadales* (OTU-442, Fig. 3) (Zhang *et al*., 2006; Besemer *et al*., 2009). On the other hand, D-LT biofilms were dominated by ciliates and purple non-sulfur *Alphaproteobacteria* and uncultured *Betaproteobacteria* affiliated to *Methylibium petroleiphilum* (Fig. 3 and Fig. 6).

On the basis of these structural differences in the dark biofilm due to warming, a shift on biofilm functioning would be expected, but only subtle changes were observed. The heterotrophic functional fingerprint in dark biofilms was characterized by the use of carboxylic acids, polymers and amino acids, and the dissimilarity between D-LT and D-HT was low (Table 3, Fig. 5). There was not any tight relationship between prokaryote community composition and functioning (Fig. 6). However, there was an increase in functional richness and diversity under warming conditions (D-HT, Table 4) due to the use of extra substrata (i.e. L-threonine, α-D-lactose, and α-ketobutyric, data not shown). The use of a broader number of substrates in D-HT biofilms might be the consequence of intense rotifer grazing pressure, resulting in a greater availability of organic matter resources (Risse-Buhl *et al*., 2012).

Temperature effects on light-grown biofilms

Under illumination, the 2°C increase also enhanced biofilm colonization by rotifers and prevented the development of ciliates to high densities, as found in dark conditions, but prokaryote densities were not significantly affected. The minor effect of rotifer grazing on prokaryote densities in L-HT conditions could be due to the following: (i) the abundant algal biomass (Fig. 1) and the extracellular accumulation of polymeric substances derived from it and/or the formation of aggregates/microcolonies protecting bacteria from grazing (Lock, 1993; Langenheder and Jürgens, 2001), and (ii) the effect of rotifer grazing upon bacterial cells is masked due to the greater bacterial growth under light and warming conditions (Díaz-Villanueva *et al*., 2011). The grazing pressure may also impair the physical structure of biofilms (Wey *et al*., 2008) as shown by the reduced spatial complexity in L-HT biofilms (Fig. 7). On the other hand, when analysing the prokaryote community composition in illuminated biofilms, small differences due to temperature occurred. Bacterial composition was similar in both temperature treatments and dominated by *Cyanobacteria* and *Alphaproteobacteria*. Most populated OTUs within the *Alphaproteobacteria* affiliated to *Rhodospirillaceae* and *Rhodobacteraceae*, two families that include a large number of photoheterotrophic representatives that could benefit from illumination conditions. The increase in the relative abundance of cyanobacterial sequences at higher temperature may be explained by their better competitiveness – and a decrease in biofilm photosynthetic efficiency – caused by the warming stress (Van der Grinten *et al*., 2004; Di Pippo *et al*., 2012).

On the other hand, warming significantly affected the biofilm carbon substrate utilization profile as shown by the large dissimilarity between L-LT and L-HT (Fig. 5, Table 3). In the case of L-HT biofilms, several OTUs affiliated to *Alphaproteobacteria* and *Cyanobacteria* (affiliated to *Oscillatoria*) showed a significant link to the use of carbohydrates (Fig. 6B). Specifically, biofilms under L-HT conditions were characterized by the use of D-mannitol, and specific OTUs from L-HT (OTU-309, OTU-30, OTU-114) significantly correlated to the use of this carbon substrate. It has been reported that *Oscillatoria* species are able to metabolize carbohydrates, including D-mannitol, glucose, lactose, fructose and methylerythritol phosphate according to the metabolic database METACYC (http://metacyc.org) (Richardson *et al*., 2009). Also, although the use of carboxylic acids was not specific for any biofilm community (Fig. 6), several carboxylic acids were specially used in L-HT biofilms, as shown by the correlation between cyanobacterial OTUs (OTU-279, OTU-308, OTU-114) and OTU-309 (affiliated to *Rhodobacter*, Fig. 3), and the use of D-glucosaminic and α-ketobutyric

acids. The use of these compounds might be related to the availability of specific photosynthetic exudates and/or extracellular polymeric substances. It has been shown that changes in light and temperature can determine changes in the composition of capsular polysaccharides and increases in the production of extracellular polymeric substances (Di Pippo *et al*., 2012). Common photosynthetic exudates include amino acids, organic acids, sugars and sugar-alcohols (Watanabe *et al*., 2008; Stengel *et al*., 2011). Recently, Taylor and colleagues (2013) demonstrated the utilization of algal produced extracellular polymeric substances by bacteria (especially *Alphaproteobacteria* and *Gammaproteobacteria*) in marine microphytobenthic biofilms. Also, the significant increase in the leucine-aminopeptidase in biofilms at L-HT may indicate a greater decomposition of proteinaceous compounds excreted by primary producers (Ylla *et al*., 2009; Díaz-Villanueva *et al*., 2011), as well as a decrease in the decomposition of polysaccharides. These functional responses might indicate a preference for using peptides (C and N sources) over polysaccharides (C source exclusively) when available. Overall, the functional heterotrophic response of illuminated biofilms to warming might be largely influenced by changes in primary producers.

Conclusions

Our results indicate that in dark-grown biofilm, an increase in 2°C determines significant changes in the prokaryote community composition but few changes in the functional outcome, except an increase in functional diversity. These changes might be mainly due to the higher density of rotifers and their potential grazing upon other biofilm members, thus altering the overall biofilm structure. Although rotifers also increased in illuminated biofilms, their effect was buffered due to both the higher complexity of biofilm matrix and the higher bacterial growth under these conditions. In light-grown biofilms, warming also determines changes in the functional outcome mainly due to readily available carbon substrates from primary producers that stimulate and enrich bacterial species specialized in the use of some carbohydrates and organic acids. These results may suggest a functional redundancy in dark-grown biofilms, where changes in the bacterial community composition did not affect the overall biofilm heterotrophic functioning. In contrast, greater metabolic versatility is suggested in light-grown biofilms as deduced by its adaptation to changes in organic matter availability without major changes in community composition, as has been described for bacterioplankton communities (Comte and del Giorgio, 2011). Biofilms grown under illumination are more complex and autoregulated (Romaní *et al*., 2004) since they have major availability of organic matter, as is indicated by the higher activities of extracellular enzymes involved in carbon, nitrogen and phosphorus organic compounds. These characteristics might determine a more buffered response of community composition in light- than in dark-grown biofilms.

A second conclusion is related to the fact that warming effect was only evident in mature biofilms, suggesting that most changes are due to interactions among biofilm members growing at different rates and/or changes in the physical structure of the biofilm (e.g. increased thickness under warming; Díaz-Villanueva *et al*., 2011) occurring as biofilm develops. Biofilms are complex biotic assemblages behaving as microecosystems with structural and trophic interactions (Besemer *et al*., 2009; Risse-Buhl *et al*., 2012). When submitted to any environmental stress, the biofilm response is modulated by interactions between the different biofilm constituents, responding as a community rather than as an assemblage of individual cells or organisms (Remis *et al*., 2010). Assuming that biofilms are a consortium of different organisms in a fragile equilibrium, only a minute change in temperature (i.e. 2°C) determines pronounced changes on biofilm structure and functioning, especially when warming is applied from initial colonization stages. Our results suggest that the thermal tolerance window needed to modify bacterial community composition and functioning in young biofilms is wider than 2°C, but that this thermal tolerance window becomes narrower at higher complexity levels (mature biofilm). The observed response is mainly due to interactions that may modify the biofilm microenvironment (i.e. changing available resources; Pekkonen and Laakso, 2012). This is similar to what was described for Antarctic ecosystems (Pörtner, 2006), where narrowest tolerance windows were shown at highest functional levels (from molecules to ecosystem). This has two consequences depending on our interest in studying biofilm dynamics and function: (i) as engineers, special attention should be taken to elucidate how small temperature changes affect biofilm biotechnological potential (Subashchandrabose *et al*., 2011), and (ii) as ecologists dealing with predictions under climate change scenarios, focus should be put on the biofilm as a whole (including structure and functioning) to investigate changes in its metabolic functioning and how these changes affect ecosystem nutrient cycling. Extrapolation of results from this cultured-based experiment to natural aquatic ecosystems must be done with caution. We should be aware that conclusions have been obtained from a specific laboratory experiment carried out in a temperature range of 15–17°C (simulating a 2°C increase in ambient temperature), oligotrophic conditions and using a defined inoculum community. Since biofilm metabolism response to temperature is not linear

(Boulêtreau *et al*., 2012), a different response level to that observed here would be expected when working at different temperature ranges.

Experimental procedures

Experimental set-up

Biofilm colonization was analysed in laboratory microcosms submitted to four different treatments: L-LT, L-HT, D-LT and D-HT. Sand-blasted glass tiles (1 cm^2) were used as substrata for biofilm growth. Tiles (60–70) were placed at the bottom of sterile glass jars (19 cm in diameter, 9 cm high). Each jar (or microcosm) was considered a replicate and three jars were established for each treatment. Microcosms were filled with 1.5 l of filter-sterilized river water (0.2 μm pore size diameter nylon filter, Whatman, Kent, UK) that was recirculated using a submersible pump (Pico 300, 230 V, 50 Hz, 4.5 W, Hydor srl, Bassano del Grappa, Italy). River water was obtained from an oligotrophic third-order forested stream in three occasions during the experiment. Water was collected from the same site and preserved filtered (0.2 μm pore size diameter nylon filter, Whatman) and at 4°C. During the study, the stream was at baseflow conditions and mean nutrient content was of 21.89 ± 4.56 μg l^{-1} $P\text{-}PO_4$, 154.0 ± 41.7 μg l^{-1} $N\text{-}NO_3$ and 4.75 ± 0.03 mg l^{-1} of dissolved organic carbon. Mean river water temperature was of 14.5°C. To promote biofilm colonization of the glass substrata, five cobbles collected from the same stream site were scrapped, and the resulting biomass suspension was used as a unique inoculum for all the experimental microcosms. This initial suspension (15 ml) had approximately 17 μg ml^{-1} of chlorophyll-*a* concentration. Microcosms were maintained unaltered for 10 days, and after this period the water from each microcosm was replaced every 3–4 days by fresh filter-sterilized river water to prevent nutrient depletion and maintain constant nutrient conditions for all the experiment. The replacing water was previously adapted at the corresponding treatment temperature. Water chemistry (dissolved oxygen, pH, conductivity, phosphate, nitrate and dissolved organic carbon) was periodically monitored in all microcosms until completion of the experiment using specific probes and standard methods (see Ylla *et al*., 2009). Along the incubation period, conductivity, pH and dissolved oxygen remained fairly constant in the range of 201–258 μS cm^{-1}, 7.2–7.7 and 8.05–9.59 mg l^{-1} respectively. Each 3–4 days, phosphate content within the microcosms decreased (to 2.9–6.2 μg l^{-1} and to 4.4–4.6 μg l^{-1} in light and dark conditions, respectively), dissolved organic carbon increased in the light treatments (to 4.83–5.89 mg l^{-1}), and nitrate remained stable.

The two temperature regimes were obtained using two different incubators (SCLAB Model PGA-500, Sistemas de Laboratorio S.L., Barcelona, Spain). Water temperature fluctuations were monitored using temperature data loggers (ACR SmartButton Logger, MicroDAQ) that were immersed within the microcosms along the incubation time (35 days). The high temperature treatments were at 17.21 ± 0.51°C (day) and 16.50 ± 0.17°C (night), and the low temperature treatments were at 15.10 ± 0.81°C (day) and 14.16 ± 0.44°C (night), with $n = 6020$ for each temperature treatment. Thus, the temperature difference between treatments was approximately 2°C (2.11 and 2.34 for day and night respectively). Day–night temperature differences were imposed to simulate the daily fluctuations in stream water. Light treatment was accomplished by exposing the growing biofilms to a light irradiance (photosynthetic active radiation) of 150 μE m^{-2} s^{-1} (fluorescent lamps, 12 h). Dark microcosms were protected from light by wrapping the incubating jars with black opaque plastic bags and aluminium foil.

Algae, prokaryote, ciliate and rotifer colonization

Biofilm biomass of primary producers was estimated from chlorophyll-*a* concentration on days 4, 7, 10, 14, 28 and 35 of incubation. Pigment extraction was accomplished by submersion of one glass tile from each microcosm into 90% acetone for 12 h in the dark at 4°C. To ensure complete extraction of pigments, samples were further sonicated for 2 min in a sonication bath (Selecta S.A.). Chlorophyll-*a* concentration of filtered extracts (fibreglass GF/C, Whatman) was determined in a Shimadzu UV-1800 spectrophotometer (Shimadzu Corporation, Kyoto, Japan).

Prokaryote, ciliate and rotifer densities were measured on days 2, 4, 7, 10, 14, 28 and 35 of incubation. For prokaryotic cell density, one glass tile from each microcosm was submerged in 5 ml of sterilized stream water, and the microorganisms were removed with a sterile cell scraper and by sonication for 2 min. Counting slides for bacteria were prepared by filtering the whole suspension through black polycarbonate filters (Poretics, 0.2 μm pore size) after staining for 10 min with 2% (V/V) DAPI (4,6-diamidino-2-phenylindole). Counting was carried out at 1000 × magnification in a Nikon E600 epifluorescence microscope (Nikon Corporation, Tokyo, Japan). Ciliate and rotifer counts were carried out on live specimens the same sampling day. One tile from each microcosm was scraped (sterile cell scraper) in 3 ml of sterilized stream water. The whole sample was collected in an Eppendorf tube and observed using a well slide under an optical microscope (100 × Nikon eclipse 80i).

Prokaryotic community composition and quantification

Prokaryotic community composition was determined using different culture-independent molecular approaches on young (7 days old) and mature (28 days old) biofilm samples. One tile from each microcosm was scraped and the recovered biomass suspended in 1 ml of filter-sterilized and autoclaved stream water. The biofilm extraction used as inoculum for the experiment was also analysed. These suspensions were stored at −30°C until processing.

DNA extraction, conventional and quantitative polymerase chain reaction (PCR). DNA from biofilm material was extracted according to Gabarró and colleagues (2012). DNA concentration in final extracts was quantified by fluorometry using QUBIT (Invitrogen Inc., Carlsbad, CA, USA). DNA extracts were stored at −80°C until use. Conventional amplification of bacterial 16S rRNA gene was performed using the universal primer pair 357F-907R for the Domain Bacteria (Lane, 1991). Amplicons from archaeal 16S rRNA genes suitable for further fingerprinting analyses were obtained after nested PCR reactions following Llirós and colleagues (2008). PCR amplification and confirmation of amplicons was carried

out using the same systems and conditions as previously described (Llirós *et al*., 2008; Ylla *et al*., 2009).

Copy numbers of bacterial, crenarchaeal and thaumarchaeal 16 s rRNA gene were determined in DNA extracts from biofilm samples by qPCR using the conditions described in Trias and colleagues (2012). PCR efficiency ranged between 80% and 90% with r^2 values > 0.99. Negative controls resulted in undetectable values in all cases. To detect possible inhibitory effects, 10^5 copies of a cloned sequence in the pGEM-T Easy plasmid (Promega Biotech Ibérica SL, Madrid, Spain) were mixed with each DNA extract and quantified with plasmid-specific primers T7 and SP6. The obtained cycle thresholds were not significantly different from those obtained when quantifying the clone alone.

Denaturing gradient gel electrophoresis and bands processing. Bacterial and archaeal 16S rRNA gene amplicons were analysed by DGGE (Muyzer *et al*., 1993). DGGE system and conditions, as well as excision, elution and sequencing of selected representative and discrete DGGE bands of different melting types, was done as described in Llirós and colleagues (2008). Within each treatment, bands located at the same position were considered the same phylotype, but at least two bands at the same position were excised and analysed independently to confirm identity. Gel image capture and analysis of fingerprint similarity among treatments were carried out as detailed in Ylla and colleagues (2009). Bacterial and archaeal 16S rRNA gene fragment sequences obtained from DGGE bands were chimera-checked, trimmed, aligned and clustered into OTUs using MOTHUR (Schloss *et al*., 2009). Representative sequences for each OTU were classified according to SILVA reference taxonomy using MOTHUR and compared for closest relatives in the National Center for Biotechnology Information (NCBI) online database (http://www.ncbi.nlm.nih.gov/blast/) using the BLASTN algorithm tool (Altschul *et al*., 1990).

Pyrosequencing, sequence processing and phylogenetic community analyses. Samples for 454 pyrosequencing were obtained after pooling equal amounts of DNA extracts (three independent samples) from mature biofilms grown under different treatments and processed as composite samples. These samples were analysed by tag-encoded FLX-titanium amplicon pyrosequencing at Research and Testing Laboratory (RTL, Lubbock, TX, USA). Briefly, composite DNA extracts from each treatment were used as template in PCR reactions using primers 341F/907R targeting the V3–5 regions of the bacterial 16 s rRNA gene complemented with 454-adapters and sample-specific barcodes. Raw sequence dataset was pre-processed in RTL facilities in order to reduce noise and sequencing artefacts as previously described (Dowd *et al*., 2008). Pyrotags were then demultiplexed according to sample barcodes and quality-filtered excluding sequences with quality scores < 30, with lengths < 250 bp or > 700 bp, and with uncorrectable barcodes, ambiguous bases and with homopolymers > 6 nt using QIIME (Caporaso *et al*., 2010a). Chimera detection and sequence clustering into OTUs were done using USEARCH (Edgar, 2010). Singletons were removed from further analysis. Representative sequences from each OTU were aligned to the Greengenes imputed core reference alignment (DeSantis *et al.,* 2006) using PYNAST (Caporaso *et al*., 2010b). Taxonomical assignments for each OTU were carried out using the RDP classifier (Wang *et al.,* 2007) retrained with the October 2012 Greengenes taxonomy database (12_10, http://greengenes.secondgenome.com). For community analysis, the number of sequences in each sample was normalized by randomly selecting a subset of 1600 sequences from each sample to standardize sequencing effort across samples and to minimize any bias due to different number of total sequences. QIIME was also used to calculate α-diversity indicators of richness (observed richness and Chao1) and diversity (Shannon) for bacterial communities grown under different conditions, and to calculate community similarity among treatments (β-diversity) using unweighted and weighted UniFrac distances (Lozupone and Knight, 2005). The robustness of Unweighted Pair Group Method with Arithmetic Mean (UPGMA) sample clustering according to UniFrac distances was assessed by jackknifing a subset of 1000 sequences from each sample to create bootstrapped trees. Relative abundance of most populated OTUs (> 100 members) across treatments was obtained using QIIME (OTU heatmap script) and visualized as a bubble plot using bubble.pl (http://www.cmde.science.ubc.ca/hallam/bubble.php).

Nucleotide sequence accession numbers. 16S rRNA sequences obtained from DGGE fingerprints were deposited in the GenBank database under accession numbers KF041009–KF041037 (archaea) and KF041038–KF041071 (bacteria). Pyrosequencing data from this study have been deposited in the NCBI via the Biosample Submission Portal (http://www.ncbi.nlm.nih.gov/biosample/) under accession numbers SAMN02144327-31.

Biofilm function

Extracellular enzyme activities of β-D-1,4-glucosidase, phosphatase and leucine-aminopeptidase were measured on biofilm from days 2, 4, 7, 10, 14 and 28 of incubation following the procedure described in Ylla and colleagues (2009), using one glass substrata per microcosm and sampling date. Samples were incubated (1 h) in the appropriate incubator to maintain the same experimental temperature. Fluorescence was measured at 365/455 nm and 364/445 nm excitation/emission for MUF (methylumbelliferone) and AMC (aminomethylcoumarin), respectively (fluorometer Kontron SFM 25, Munich, Germany), and results were expressed as nmol MUF or AMC cm^{-2} h^{-1}.

Functional diversity. Biolog Ecoplates™ microplates (Biolog Inc., Hayward, CA, USA) were used in order to determine the differences in heterotrophic metabolic capabilities. Each microplate contains three replicate wells of 31 carbon sources assigned to chemical groups as polymers, carbohydrates, carboxylic acids, amino acids and amines (Choi and Dobbs, 1999). At days 7 and 28 of biofilm colonization, a glass tile was collected from each microcosm, and the biofilm was extracted with a cell scrapper and 2 ml of Ringer solution, and further homogenized by 2 min sonication. Microplates were inoculated under sterile conditions (130 µl of the biofilm extract to each well) and incubated at the correspondent temperature treatment conditions, in dark for

6 days. After incubation, optical density at 590 nm was recorded using a microplate reader (SynergyTM 4, BioTek, Winooski, VT, USA). From each microplate, functional richness (number of positive wells) and microbial community functional diversity (Shannon's diversity index) were calculated.

Photosynthetic efficiency. Two randomly selected colonized glass tiles per microcosm were used to determine the biofilm photon yield of mature biofilms as a measure of the photosynthetic efficiency of the community (Schreiber *et al*., 2002). Mean biofilm photon yield and photon yield of the main photosynthetic groups were measured by a phytoPAM (pulse amplitude modulated) fluorometer (Heinz Walz GmbH with the emitter-detector unit PHYTO-EDF, Effeltrich, Germany) following the procedure described by Ylla and colleagues (2009).

Biofilm structure

To assess for changes in biofilm structure due to the light and temperature treatments, SEM observations were performed. Samples for SEM (one glass tile from each treatment collected after 28 days of incubation) were fixed immediately after sampling with 2.5% glutaraldehyde in 0.1 M cacodilate buffer, pH 7.2–7.4. Samples were then subjected to serial dehydration baths (from 65% to 100% ethanol) and further dried by the critical point method with CO_2. Samples were finally coated with gold using a sputtering diode and observed under a Zeiss DSM 960 scanning electron microscope (Oberkochen, Germany).

Data analyses

The effects of temperature and light conditions on chlorophyll-*a* concentration, prokaryote, ciliate and rotifer densities, and extracellular enzyme activities throughout biofilm formation, were analysed by repeated measures analysis of variance (two-way RM-ANOVA, temperature and light as fixed factors) using SPSS (IBM Corp., Armonk, NY, USA). The effects of biofilm age (young/mature biofilm), temperature and light conditions on bacteria and *Crenarchaeota-Thaumarchaeota* gene copies, and heterotrophic functional diversity and richness, were analysed by a multivariate three-way ANOVA. Difference between treatments for photosynthetic efficiency on the mature biofilm was analysed by a one-way ANOVA. All response variables (x) were transformed with log(x) except chlorophyll-*a* transformed log(x + 1) to improve the homoscedasticity and heterogeneity of variance.

To analyse bacterial diversity, similarity patterns were calculated with the Sorensen coefficient (Murray *et al*., 1996). Dendrograms were built based on the complete linkage method with the PRIMER 6 and PERMANOVA + programme (version 6, Primer-E, Plymouth, UK, 2006). Primer-E was also used to compute similarity percentages (SIMPER) to highlight and identify specific organic substrates used by each biofilm community. The test performed was a two-way SIMPER analysis with the normalized absorbance (divided by average well colour development) for each substrate of the Biolog EcoPlates. The similarity matrix was built using Bray–Curtis distances to reveal (i) differences between young and mature biofilm, and (ii) differences between treatments for the mature biofilm. Results from these analyses were plotted in an nMDS graphical layout.

The relationship between prokaryote community composition (using the 22 most abundant OTUs, Fig. 3) and the biomass of the different groups (chlorophyll-a, prokaryote, ciliate, rotifer), and the carbon substrate utilization profile by grouping the five carbon source types (carbohydrates, polymers, carboxylic acids, amino acids, amines), was analysed by redundancy analyses (RDA). Before being included in the analysis, all metrics were transformed as follows: biomass data using log10 (x + 1) transformation, Biolog data were normalized by dividing absorbance by average well color development, and the relative abundance of bacterial phyla using angular transformation. The redundancy analysis was performed with CANOCO software, version 4.5. Furthermore, Pearson correlations between the 31 carbon substrates and the 22 abundant OTUs were carried out to find individual relationships between carbon substrate utilization and prokaryote groups. Pearson's correlation analyses were performed with SPSS, and the differences were considered to be significant at $P < 0.05$.

Acknowledgements

This study was funded by the Spanish Ministry of Economy and Competitiveness, project FLUMED-HOTSPOTS (CGL2011–30151-C02-01). V. Díaz Villanueva participated in this project supported by FONCYT (Argentina) (PICT-2007-01747) and CONICET (PIP 114–201101-00304).

References

Altschul, S.F., Gish, W., Miller, W., Myers, E.W., and Lipman, D.J. (1990) Basic local alignment search tool. *J Mol Biol* **215:** 403–410.

Augspurger, C., Gleixner, G., Kramer, C., and Küsel, K. (2008) Tracking carbon flow in a 2-week-old and 6-week-old stream biofilm food web. *Limnol Oceanogr* **53:** 642–650.

Besemer, K., Hödl, I., Singer, G., and Battin, T.J. (2009) Architectural differentiation reflects bacterial community structure in stream biofilms. *ISME J* **3:** 1318–1324.

Besemer, K., Peter, H., Logue, J.B., Langenheder, S., Lindström, E.S., Tranvik, L.J., and Battin, T.J. (2012) Unraveling assembly of stream biofilm communities. *ISME J* **6:** 1459–1468.

Boulêtreau, S., Salvo, E., Lyautey, E., Mastrorillo, S., and Garabetian, F. (2012) Temperature dependence of denitrification in phototrophic river biofilms. *Sci Total Environ* **416:** 323–328.

Caporaso, J.G., Kuczynski, J., Stombaugh, J., Bittinger, K., Bushman, F.D., Costello, E.K., *et al*. (2010a) QIIME allows analysis of high-throughput community sequencing data. *Nat Methods* **7:** 335–336.

Caporaso, J.G., Bittinger, K., Bushman, F.D., DeSantis, T.Z., Andersen, G.L., and Knight, R. (2010b) PyNAST: a flexible tool for aligning sequences to a template alignment. *Bioinformatics* **26:** 266–267.

Choi, K.-H., and Dobbs, F.C. (1999) Comparison of two kinds of Biolog microplates (GN and ECO) in their ability to

distinguish among aquatic microbial communities. *J Microbiol Methods* **36:** 203–213.
Church, M.J., Wai, B., Karl, D.M., and DeLong, E.F. (2010) Abundances of crenarchaeal *amoA* genes and transcripts in the Pacific Ocean. *Environ Microbiol* **12:** 679–688.
Comte, J., and del Giorgio, P.A. (2011) Composition influences the pathway but not the outcome of the metabolic response of bacterioplankton to resource shifts. *PLoS ONE* **6:** e25266. doi:10.1371/journal.pone.0025266.
Degerman, R., Dinasquet, J., Riemann, L., Sjöstedt de Luna, S., and Andersson, A. (2013) Effect of resource availability on bacterial community responses to increased temperature. *Aquat Microb Ecol* **68:** 131–142.
DeSantis, T.Z., Hugenholtz, P., Larsen, N., Rojas, M., Brodie, E.L., Keller, K., *et al*. (2006) Greengenes, a chimera-checked 16S rRNA gene database and workbench compatible with ARB. *Appl Environ Microbiol* **72:** 5069–5072.
Díaz-Villanueva, V., Font, J., Schwartz, T., and Romaní, A.M. (2011) Biofilm formation at warming temperature: acceleration of microbial colonization and microbial interactive effects. *Biofouling* **27:** 59–71.
Di Pippo, F., Ellwood, N.T.W., Guzzon, A., Siliato, L., Micheletti, E., De Philippis, R., and Albertano, P.B. (2012) Effect of light and temperature on biomass, photosynthesis and capsular polysaccharides in cultured phototrophic biofilms. *J Appl Phycol* **24:** 211–220.
Dowd, S.E., Callaway, T.R., Wolcott, R.D., Sun, Y., McKeehan, T., Hagevoort, R.G., and Edrington, T.S. (2008) Evaluation of the bacterial diversity in the feces of cattle using 16S rDNA bacterial tag-encoded FLX amplicon pyrosequencing (bTEFAP). *BMC Microbiol* **8:** 125–132.
Edgar, R.C. (2010) Search and clustering orders of magnitude faster than BLAST. *Bioinformatics* **26:** 2460–2461.
Findlay, S. (2010) Stream microbial ecology. *J N Am Benthol Soc* **29:** 170–181.
Frossard, A., Gerull, L., Mutz, M., and Gessner, M.O. (2012) Disconnect of microbial structure and function: enzyme activities and bacterial communities in nascent stream corridors. *ISME J* **6:** 680–691.
Früh, D., Norf, H., and Weitere, M. (2011) Response of biofilm-dwelling ciliate communities to enrichment with algae. *Aquat Microb Ecol* **63:** 299–309.
Fuhrman, J.A., Hewson, I., Schwalbach, M.S., Steele, J.A., Brown, M.V., and Naeem, S. (2006) Annually reoccurring bacterial communities are predictable from ocean conditions. *Proc Natl Acad Sci USA* **103:** 13104–13109.
Gabarró, J., Ganigué, R., Gich, F., Ruscalleda, M., Balaguer, M.D., and Colprim, J. (2012) Effect of temperature on AOB activity of a partial nitritation SBR treating landfill leachate with extremely high nitrogen concentration. *Bioresour Technol* **126:** 283–289.
Gilbert, J.J., and Jack, J.D. (1993) Rotifers as predators on small ciliates. *Hydrobiology* **255–256:** 247–253.
Gomez-Gil, B., Thompson, F.L., Thompson, C.C., and Swings, J. (2003) Vibrio rotiferianus sp. nov., isolated from cultures of the rotifer Brachionus plicatilis. *Int J Syst Evol Microbiol* **53:** 239–243.
Guenet, B., Danger, M., Abbadie, L., and Lacroix, G. (2010) Priming effect: bridging the gap between terrestrial and aquatic ecology. *Ecology* **91:** 2850–2861.
Henneberger, R., Moissl, C., Amann, T., Rudolph, C., and Huber, R. (2006) New insights into the lifestyle of the cold-loving SM1 euryarchaeon: natural growth as a monospecies biofilm in the subsurface. *Appl Environ Microbiol* **72:** 192–199.
Hester, E.T., and Doyle, M.W. (2011) Human impacts to river temperature and their effects on biological processes: a quantitative synthesis. *J Am Water Resour Assoc* **47:** 571–587.
IPCC. (2007) Summary for policymakers. In *Climate Change 2007: The Physical Science Basis. Contribution of Working Group I to the Fourth Assessment Report of the Intergovernmental Panel on Climate Change*. Solomon, S., Qin, D., Manning, M., Chen, Z., Marquis, M., Averyt, K.B., *et al*. (eds). Cambridge, UK and New York, NY, USA: Cambridge University Press, pp. 1–18.
Ishino, R., Iehata, S., Nakano, M., Tanaka, R., Yoshimatsu, T., and Maeda, H. (2012) Bacterial diversity associated with the rotifer *Brachionus plicatilis* sp. complex determined by culture-dependent and – independent methods. *Biocontrol Sci* **17:** 51–56.
Jackson, C.R. (2003) Changes in community properties during microbial succession. *Oikos* **101:** 444–448.
Klappenbach, J.A., Saxman, P.R., Cole, J.R., and Schmidt, T.M. (2001) rrndb: the Ribosomal RNA Operon Copy Number Database. *Nucleic Acids Res* **29:** 181–184.
Lane, D.J. (1991) 16S/23S rRNA sequencing. In *Nucleic Acid Techniques in Bacterial Systematics*. Stackebrandt, E., and Goodfellow, M. (eds). New York, NY, USA: John Wiley and Sons, pp. 115–175.
Langenheder, S., and Jürgens, K. (2001) Regulation of bacterial biomass and community structure by metazoan and protozoan predation. *Limnol Oceanogr* **46:** 121–134.
Langenheder, S., Lindström, E., and Tranvik, L.J. (2005) Weak coupling between community composition and functioning of aquatic bacteria. *Limnol Oceanogr* **50:** 957–967.
Lear, G., Anderson, M.J., Smith, J.P., Boxen, K., and Lewis, G.D. (2008) Spatial and temporal heterogeneity of the bacterial communities in stream epilithic biofilms. *Microb Ecol* **65:** 463–473.
Llirós, M., Casamayor, E.O., and Borrego, C.M. (2008) High archaeal richness in the water column of a freshwater sulfurous karstic lake along an interannual study. *FEMS Microbiol Ecol* **66:** 331–342.
Lock, M.A. (1993) Attached microbial communities in rivers. In *Aquatic Microbiology*. Ford, T.E. (ed.). Oxford, UK: Blackwell, pp. 113–138.
Lozupone, C., and Knight, R. (2005) UniFrac: a new phylogenetic method for comparing microbial communities. *Appl Environ Microbiol* **71:** 8228–8235.
Merbt, S.N., Auguet, J.C., Casamayor, E.O., and Martí, E. (2011) Biofilm recovery in a wastewater treatment plant-influenced stream and spatial segregation of ammonia-oxidizing microbial populations. *Limnol Oceanogr* **56:** 1054–1064.
Mohseni, O., and Stefan, H.G. (1999) Stream temperature/air temperature relationship: a physical interpretation. *J Hydrol* **218:** 128–141.
Murray, A.E., Hollibaugh, J.T., and Orrego, C. (1996) Phylogenetic compositions of bacterioplankton from two

California estuaries compared by denaturing gradient gel electrophoresis of 16S rDNA fragments. *Appl Environ Microbiol* **62:** 2676–2680.

Muyzer, G., and Smalla, K. (1998) Application of denaturing gradient gel electrophoresis (DGGE) and temperature gradient gel electrophoresis (TGGE) in microbial ecology. *Antonie Van Leeuwenhoek* **73:** 127–141.

Muyzer, G., de Waal, E.C., and Uitterlinden, A.G. (1993) Profiling of complex microbial populations by denaturing gradient gel electrophoresis analysis of polymerase chain reaction-amplified genes coding for 16S rRNA. *Appl Environ Microbiol* **59:** 695–700.

Neely, R.K., and Wetzel, R.G. (1995) Simultaneous use of ^{14}C and ^{3}H to determine autotrophic production and bacteria protein production in periphyton. *Microb Ecol* **30:** 227–237.

Norf, H., Arndt, H., and Weitere, M. (2007) Impact of local temperature increase on the early development of biofilm – associated ciliate communities. *Oecologia* **151:** 341–350.

Pagé, A., Tivey, M.K., Stakes, D.S., and Reysenbach, A.L. (2008) Temporal and spatial archaeal colonization of hydrothermal vent deposits. *Environ Microbiol* **10:** 874–884.

Pajdak-Stós, A., and Fialkowska, E. (2012) The influence of temperature on the effectiveness of filmanetous bacteria removal from activated sludge by Rotifers. *Water Environ Res* **84:** 619–625.

Pekkonen, M., and Laakso, J.T. (2012) Temporal changes in species interactions in simple aquatic bacterial communities. *BMC Ecol* **12:** 18. doi:10.1186/1472–6785-12-18.

Perkins, D.M., Yvon-Durocher, G., Demars, B.O.L., Reiss, J., Pichler, D.E., Friberg, N., *et al*. (2012) Consistent temperature dependence of respiration across ecosystems contrasting in thermal history. *Glob Chang Biol* **18:** 1300–1311.

Peter, H., Ylla, I., Gudasz, C., Romaní, A.M., Sabater, S., and Tranvik, L.J. (2011) Multifunctionality and diversity in bacterial biofilms. *PLoS ONE* **6:** e23225. doi:10.1371/journal.pone.0023225.

Pörtner, H.O. (2006) Climate-dependent evolution of Antarctic ecotherms: an integrative analysis. *Deep Sea Res II* **56:** 1071–1104.

Pusch, M., Fiebig, D., Brettar, I., Eisenmann, H., Ellis, B.K., Kaplan, L.A., *et al*. (1998) The role of micro-organisms in the ecological connectivity of running waters. *Freshw Biol* **40:** 453–495.

Remis, J.P., Costerton, J.W., and Auer, M. (2010) Biofilms: structures that may facilitate cell-cell interactions. *ISME J* **4:** 1085–1087.

Ricci, C., and Balsamo, M. (2000) The biology and ecology of lotic rotifers and gastrotrichs. *Freshw Biol* **44:** 15–28.

Richardson, L.L., Miller, A.W., Broderick, E., Kaczmarsky, L., Gantar, M., Stanić, D., and Sekar, R. (2009) Sulfide, microcystin, and the etiology of black band disease. *Dis Aquat Organ* **87:** 79–90.

Risse-Buhl, U., Karsubke, M., Schlief, J., Baschien, C., Weitere, M., and Mutz, M. (2012) Aquatic protists modulate the microbial activity associated with mineral surfaces and leaf litter. *Aquat Microb Ecol* **66:** 133–147.

Romaní, A.M. (2010) Freshwater biofilms. In *Biofouling*. Dürr, S., and Thomason, J.C. (eds). Oxford, UK: Wiley-Blackwell, pp. 137–153.

Romaní, A.M., Guasch, H., Muñoz, I., Ruana, J., Vilalta, E., Schwartz, T., *et al*. (2004) Biofilm structure and function and possible implications for riverine DOC dynamics. *Microb Ecol* **47:** 316–328.

Rosa, J., Ferreira, V., Canhoto, C., and Graça, M.A.S. (2013) Combined effects of water temperature and nutrients concentration on periphyton respiration – implications of global change. *Int Rev Hydrobiol* **98:** 14–23.

Schloss, P., Westcott, S., Ryabin, T., Hall, J.R., Hartmann, M., Hollister, E., *et al*. (2009) Introducing Mothur: open-source, platform-independent, community-supported software for describing and comparing microbial communities. *Appl Environ Microbiol* **75:** 7537–7541.

Schopf, S., Wanner, G., Rachel, R., and Wirth, R. (2008) An archaeal bi-species bioWlm formed by *Pyrococcus furiosus* and *Methanopyrus kandleri*. *Arch Microbiol* **190:** 371–377.

Schreiber, U., Gademann, R., Bird, P., Ralph, P.J., Larkum, A.W.D., and Kuhl, M. (2002) Apparent light requirement for activation of photosynthesis upon rehydration of desiccated beachrock microbial mats. *J Phycol* **38:** 125–134.

Singer, G., Besemer, K., Schmitt-Kopplin, P., Hödl, I., and Battin, T.J. (2010) Physical heterogeneity increases biofilm resource use and its molecular diversity in stream mesocosms. *PLoS ONE* **5:** e9988. doi:10.1371/journal.pone.0009988.

Stengel, D.B., Connan, S., and Popper, Z.A. (2011) Algal chemodiversity and bioactivity: sources of natural variability and implications for commercial application. *Biotechnol Adv* **29:** 483–501.

Subashchandrabose, S.R., Ramakrishnan, B., Megharaj, M., Venkateswarlu, K., and Naidu, R. (2011) Consortia of cyanobacteria/microalgae and bacteria: biotechnological potential. *Biotechnol Adv* **29:** 896–907.

Taylor, J.D., McKew, B.A., Kuhl, A., McGenity, T.J., and Underwood, G.J.C. (2013) Microphytobenthic extracellular polymeric substances (EPS) in intertidal sediments fuel both generalist and specialist EPS-degrading bacteria. *Limnol Oceanogr* **58:** 1463–1480.

Trias, R., García-Lledó, A., Sánchez, N., López-Jurado, J.L., Hallin, S., and Bañeras, L. (2012) Abundance and composition of epiphytic bacterial and archaeal ammonia oxidizers of marine red and brown macroalgae. *Appl Environ Microbiol* **78:** 318–325.

Van der Grinten, E., Janssen, M., Simis, S.G.H., Barranguet, C., and Admiral, W. (2004) Phosphate regime structure species composition in cultured phototrophic biofilms. *Freshw Biol* **49:** 369–381.

Vianna, M.E., Holtgraewe, S., Seyfarth, I., Conrads, G., and Horz, H.P. (2008) Quantitative analysis of three hydrogenotrophic microbial groups, methanogenic archaea, sulfate-reducing bacteria, and acetogenic bacteria, within plaque biofilms associated with human periodontal disease. *J Bacteriol* **190:** 3779–3785.

Walther, G.-R., Post, E., Convey, P., Menzel, A., Parmesan, C., Beebee, T.J.C., *et al*. (2002) Ecological responses to recent climate change. *Nature* **416:** 389–395.

Wang, Q., Garrity, G.M., Tiedje, J.M., and Cole, J.R. (2007) Naive Bayesian classifier for rapid assignment of rRNA sequences into the new bacterial taxonomy. *Appl Environ Microbiol* **73:** 5261–5267.

Watanabe, K., Imase, M., Aoyagi, H., Ohmura, N., Saiki, H., and Tanaka, H. (2008) Development of a novel artificial medium based on utilization of algal photosynthetic metabolites by symbiotic heterotrophs. *J Appl Microbiol* **105:** 741–751.

Wey, J.K., Jürgens, K., and Weitere, M. (2012) Seasonal and successional influences on bacterial community composition exceed that of protozoan grazing in River Biofilms. *Appl Environ Microbiol* **78:** 2013–2024.

Wey, J.K., Scherwass, A., Norf, H., Arndt, H., and Weitere, M. (2008) Effects of protozoan grazing within river biofilms under semi-natural conditions. *Aquat Microb Ecol* **52:** 283–296.

Ylla, I., Romaní, A.M., and Sabater, S. (2012) Labile and recalcitrant organic matter utilization by River Biofilm under increasing water temperature. *Microb Ecol* **64:** 593–604.

Ylla, I., Borrego, C., Romaní, A.M., and Sabater, S. (2009) Availability of glucose and light modulates the structure and function of a microbial biofilm. *FEMS Microbiol Ecol* **69:** 27–42.

Zhang, K., Choi, H., Dionysiou, D.D., Sorial, G.A., and Oerther, D.B. (2006) Identifying pioneer bacterial species responsible for biofouling membrane bioreactors. *Environ Microbiol* **8:** 433–440.

Ziegler, S.E., Lyon, D.R., and Townsend, S.L. (2009) Carbon release and cycling within epilithic biofilms in two contrasting headwater streams. *Aquat Microb Ecol* **55:** 285–300.

Supporting information

Additional Supporting Information may be found in the online version of this article at the publisher's web-site:

Fig. S1. Negative images of bacterial 16S rRNA gene DGGE fingerprints obtained from biofilms samples after (A) 7 days and (B) 28 days of incubation. For each treatment, triplicate samples were analysed. Excised and sequenced bands are indicated and numerically labelled (arrowheads). Green arrowheads indicate bands which sequences affiliated to *Cyanobacteria* (see Table S1). Red arrowheads indicate bands which yielded unspecific products.

Fig. S2. (A) Clustering of samples based on unweighted UniFrac distances. (B) Clustering of samples after filtering cyanobacterial OTUs from the dataset (71 out of 496 total OTUs). In all dendrograms, red-coloured nodes indicate a 75–100% support after rarifying the UPGMA trees using a random subset of 1000 sequences per sample (Jackknife test in QIIME). Subsampling of the *Cyanobacteria*-free dataset was run at 800 sequences since filtering removed a large amount of sequences from samples incubated under illumination (L-LT and L-HT). INO: inoculum; D: dark; L: light; LT: low temperature; HT: high temperature.

Fig. S3. Clustering of samples according to Bray–Curtis similarity index of (A) the relative abundance of bacterial taxa (angular transformed) calculated from pyrosenquencing dataset and (B) the similarity of DGGE fingerprints based on Jaccard coefficient of 28-day biofilms (triplicate samples for each treatment, see Fig. S1). INO: inoculum; L: light; D: dark; LT: low temperature; HT: high temperature.

Fig. S4. Phylogenetic tree of partial 16S rRNA gene sequences obtained from pyrosequencing analysis (OTUs > 100 members, in red) and from DGGE fingerprinting (in blue). The tree was calculated using the neighbour-joining method [1] and Jukes–Cantor algorithm [2]. Significant bootstrap values (≥ 50 %) from 1000 replicates are shown at branch nodes. Scale bar indicates 3% estimated sequence divergence. All ambiguous positions were removed for each sequence pair. Evolutionary analyses were conducted in MEGA5 [3].

Fig. S5. Negative images of crenarchaeotal16S rRNA gene DGGE fingerprints obtained from biofilms samples after 7 and 28 days of incubation. For each treatment, triplicate samples were analysed (see *Experimental procedures*) with the exception of D-HT (28 days) and L-HT (7 days) from which universal archaeal amplicons were obtained in only two of the three replicas. Excised and sequenced bands are indicated (arrowheads). All sequences affiliated to Soil Group 1.1b (*Thaumarchaeota*) and distributed into 5 OTUs (see Table S3) as indicated by band number and colour code. Orange (OTU-1, 18 members), green (OTU-2, 4 members), red (OTU-3, 2 members), white (OTU-4, singleton) and blue (OTU-5, 3 members). See Table S4 for further details on OTU affiliation, OTU members and representative sequences. Ld: ladder.

Table S1. BLAST hit of partial 16S rRNA gene sequences obtained from DGGE bands (see Fig. S1).

Table S2. Richness and diversity indices of biofilm bacterial communities under different treatments calculated from pyrosequencing data (28-day biofilms).

Table S3. Number of OTUs affiliated into each bacterial phyla (class for *Proteobacteria*) and relative contribution (in %) to the total number of OTUs. Taxa are named according to Greengenes database. Rare taxa (*) accounted for an 8% of total diversity.

Table S4. Information of archaeal OTUs identified from DGGE analysis. OTU definition and identification of representative sequences were carried out using MOTHUR v.1.24 (Schloss *et al.*, 2009; see *Experimental procedures* for details). Sequences codes refer to bands shown in Fig. S5.